Determining the Basement Fault Structure of the Hogback Monocline in Northwest NM Using Fracture Patterns and Geomechanical Modeling

By

Van Madrid Lancaster

Fort Lewis College

Undergraduate Research

Department of Geosciences

April 27, 2019

Introduction

Monoclines are caused from movement of normal or reverse faults that cause forced folding or fault propagation folding in the overlying stratigraphy (Mitra & Mount, 1998).

Monoclines and the fault structures underlying them are well understood when linear but not when there are bends in the trend of the monocline's axis. Although basement involved structures have been studied for over a century, the underlying faults system geometry is a mystery in places where monoclines deviate from a linear trend (Mitra & Mount, 1998). Also, only 2D concepts and models exist, and no 3D models exist of the fault systems in these places.

On the Colorado Plateau, monoclines with bends are quite prevalent. Between Waterflow, NM and Durango, CO along the Hogback Monocline, there are four such examples of these bends (Lorenz, et al., 2003), one of which has been selected for the study area of this project. These bends have been described as en echelon in geometry and also are used as evidence for compressional stress environments (Lorenz, et al., 2003; Kelley, 1955). Through the collection of field data of fracture and bedding orientation, the geometry of the monocline's structure was analyzed and compared to models.

The significance of this modeling is due to its 3D nature. Modeling of these structures has never before been done in 3D. Two-dimensional models, such as cross-sections, only depict the simple geometry between the basement fault and the folded stratigraphy. Two-dimensional cross-sections depict a linear structure, but incorporating numerical modeling into the modeling process allows for a greater number of analyses to be conducted on the models' results and the outcrop.

This investigation focused on using fracture orientations seen in outcrop to assess basement geometry and orientation in relation to the structures seen at the surface. This can better the understanding of subsurface fracture orientations over a variety of positions in the structure, as well as provide important additional evidence of the timing and genesis of these fractures, the extent of fault propagation in the stratigraphic section, and the nature of deformation zones associated with these structures, all of which affect the efficiency of exploration and production in the industry (Erslev, 2009; Mitra & Mount, 1998). Through the investigation of these complex structures, industries such as petroleum and hydrology will benefit from increased understanding of basement faulting and the overlying stratigraphy. In addition to benefitting these industries, academia benefits from the increased understanding of these structures and their structural causes.

Background

Colorado Plateau

At first glance, the Colorado Plateau is a geologically simple place, but upon further inspection it becomes much more complex (*Figure 1*). It is composed of Neoproterozoic, Paleozoic, and Mesozoic stratigraphy, overlying Paleoproterozoic and Mesoproterozoic mechanically heterogeneous crystalline basement (Davis & Bump, 2009).

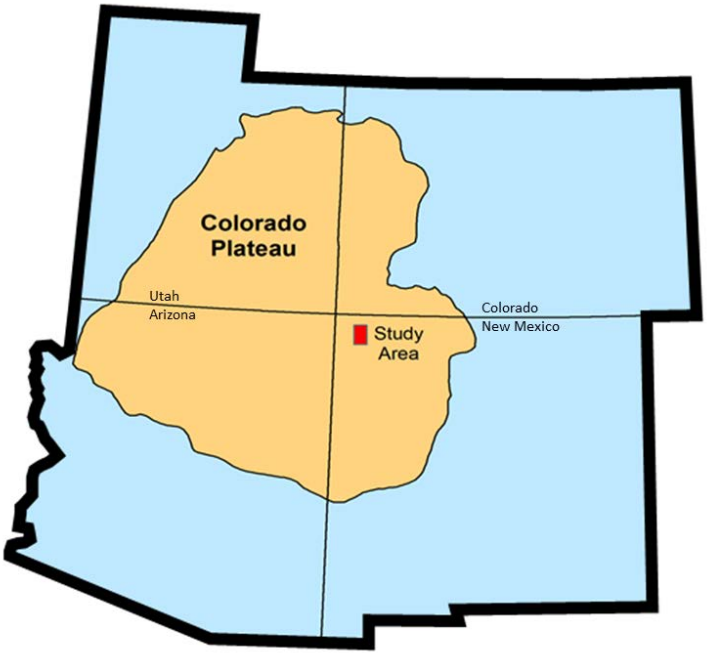

Figure 1: Delineation of the Colorado Plateau. Although it is not shown in the map, the Colorado Plateau falls between the Rocky Mountain and Basin and Range physiographic provinces.

Experiencing many orogenies, there are many individual deformation signatures on the Colorado Plateau. The different tectonic events have left their mark in various forms and features. Among these features are monoclines, and they are one of the most common features on

the plateau (Kelley, 1955). There are ten dominating structures, which are basement-cored uplifts and associated monoclines, which were formed during the late Cretaceous and the Tertiary Laramide orogeny (Davis & Bump, 2009). Besides the uplift structures, basins represent another large portion of structural deformation and represent about one-third of the plateau's area (Kelley, 1955). Nevertheless, the primary deformation appears to be in the monoclines (Kelley, 1955).

Because the Colorado Plateau has such a complex past, and various forms of deformation through different historic events, the deformation has begun to overprint. The most recent tectonic deformation event experienced by the Colorado Plateau is the Laramide orogeny. The deformation period ranged from 80-40 Ma.

Many monoclines on the Colorado Plateau are the result of at least two generations of deformation. The consensus is that the faults that slipped during the Laramide orogeny, to form the monoclines, are reactivated Neoproterozoic basement normal faults (Davis & Bump, 2009).

When looking at the Colorado Plateau zoomed out, distinct patterns are visible (*Figure 2*). These patterns are signatures of the fault orientations that have occurred from paleo-tectonism. The basement faults on the Colorado Plateau are from a period of extension during the Neoproterozoic (Davis & Bump, 2009). Through the topographic analysis of structures that overly basement faults, we see two orientations of faulting, both of which are the result of different extension regimes. These two orientations create an orthogonal grid pattern shown in Figure Above (Davis, 1978; Cather, 2003). This pattern forms a network of curvilinear and branching folds, favoring the relationship between the basement faults and overlying monoclines, rather than systems of flexural or bucklefold seen in sedimentary sequences (Davis, 1978). The directions of shortening lie perpendicular to the two groups of structures, and are as

follows: northeast-southwest and northwest-southeast (Davis & Bump, 2009). These patterns of deformation of the covering stratigraphy can be interpreted as a result of basement strain, which originated ultimately from plate tectonic stresses (Davis & Bump, 2009).

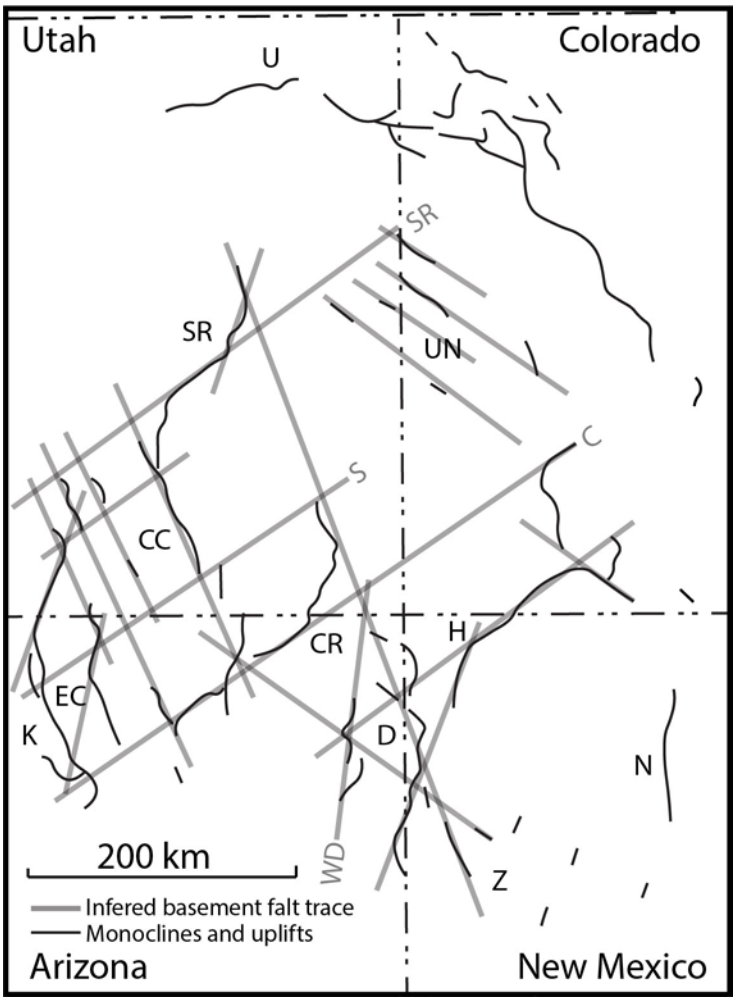

Figure 2: Delineation of major uplift structures of the Colorado Plateau and associated inferred basement fracture zone lineations (Kelley, 1955; Davis, 1978). The black lines represent structures seen at the surface and the black labels indicate their names. The grey lines represent inferred basement lineations. U = Uinta; SR = San Rafael; UN = Uncompahgre; C = Coconino; CC = Circle Cliffs; S = Snowmass; EC = Echo Cliffs; CR = Comb Ridge; H = Hogback; K = Kaibab; D = Defiance; N = Nacemiento; Z = Zuni; WD = West Defiance.

Laramide Orogeny

The Laramide orogeny was the primary cause of the deformation seen in the Colorado Plateau and invoked a northeast-southwest and northwest-southeast compression, at different periods (Davis, 1978; Davis & Bump, 2009). This compression caused syntectonic folding during movement of high angle ancient faults (Davis, 1978). These steeply dipping faults have dips between 60^{o} and 75^{o} (Miller & Mitra, 2011). Across the Colorado Plateau, a mosaic of basement blocks were uplifted by a reverse movement along these steeply dipping faults (Davis, 1978). The movement of these blocks happened differentially during folding of the monoclines (Davis, 1978). In relation to differential movement, evidence suggests that the movement of the eastern monoclines began before the uplift of the western monoclines and continued after (Kelley, 1955). These faults have also been described as master shear zones, and are rooted in the basement (Davis & Bump, 2009; Miller & Mitra, 2011).

Monoclines

A monocline is a double fold structure that has been described in many ways in the last centuries. In 1876, Gilbert described a monoclinal fold as “a double flexure connecting strata at one level with the same strata at another level”. Davis, Reynolds, and Kluth (2012) describe monoclines as step-like folds that cause otherwise horizontal strata to bend abruptly. Fossen (2010) describes monoclines as a fold with only one inclined limb. Mitra and Mount (1998) acknowledged monoclines’ relationships to compressional foreland crystalline basement faulting, and described them as occurring in long irregular chains of uplifts, where a deformation zone in the stratigraphy dissipates the fault slip and has gently dipping forelimbs and backlimbs. The relief between these forelimbs and backlimbs is directly associated with the throw the fault

experienced. On the Colorado Plateau, the uplift can reach up to two kilometers of relief (Davis & Bump, 2009). Kelley (1955) contributed the idea that monoclines are associated with regions of gentle dips, outside of the head and foot of the structure, that their length to width ratios are great, and that their geometries can be described in many ways, including gentle or steep, narrow or broad, opened or closed, level or plunging, buckled, etc. *Figure 3* clearly shows the relationship between the basement fault and the folded overlying stratigraphy, as described by numerous authors.

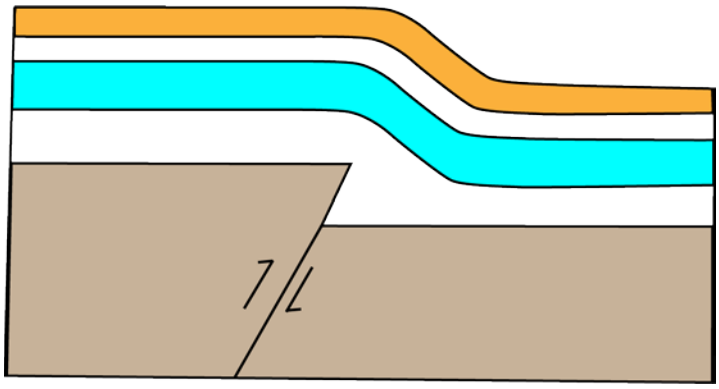

Figure 3: Simple schematic of monoclonal cross-section. Shows dissipation of fault slip into folding of the overlying layers.

The majority of evidence supports the hypothesis that compression led to the formation of the uplift structures, especially concerning monoclines of the Colorado Plateau. Kelley (1955) efficiently outlines this evidence in seven points:

> (1) Asymmetrical form of the uplifts. (2) Curving of the monoclines toward the uplifts at the terminations. (3) Small staggered and echelon folds along the crests of the uplifts. (4) Small staggered and echelon folds immediately above the heads or below the bottoms of the monoclines. (5) Sharper synclinal bends than anticlinal bends. (6) Small scission thrusts associated with the monoclines and uplifts. (7) Gradation on a regional scale between gentle monoclines and thrust faults.

These structures are described in Mitra and Mount's (1998) article as foreland basement structures, which form during compressional periods. Monoclines associated with compression are described as having shallow dipping reverse or thrust faults between 30^{o} and 45^{o} (Miller & Mitra, 2011). Whereas monoclines associated with extension are described as having steeply dipping underlying faults between 60^{o} and 75^{o} (Miller & Mitra, 2011). In the Grand Canyon region, the spatial and genetic relationships between monoclines and steeply dipping faults suggest an extensional regime, however, they are ancient reactivated faults (Davis, 1978). Even though these geometric relations resulted from an earlier period of extension, they are reactivated, and thus can have steeply dipping faults move during compression (Davis, 1978). In either case of extension or compression, the major basement faults are associated with the dipping limb of the monoclines (Davis, 1978).

Regardless of the underlying fault geometry, the deformation experienced by the sedimentary cover occurs in a triangular zone, where the units closer to the basement experience deformation within a narrower zone than the units closer to the surface based on Erslev (2009) trishear models. The distribution of secondary fractures, their orientations, and the width of the deformation zone, are all indications of the underlying major fault geometry (Miller & Mitra, 2011). The nature of deformation is primarily controlled by mechanical stratigraphy (Mitra & Mount, 1998). This mechanical stratigraphy – whether it is original or from diagenetic processes – determines fracture characteristics, thus even when the same stress is imposed on two different units, their fractures may differ (Lorenz et al., 2003).

San Juan Basin

Lying on the southeastern portion of the Colorado Plateau is the San Juan Basin. The basin's perimeter consists of monoclines and uplifts. The tectonism that influenced the formation of the basin occurred in three distinct phases of uplift and subsidence (Cather, 2003). Evidence of these phases consists of sedimentation, thickness of sediment packages, angular unconformities, and geochronology (Cather, 2003). The relationship between the monoclines and the stratigraphy also suggests movement was not everywhere uniform (Kelley, 1955). In addition to differential movement along the basement faults, there were also different directions of movement along these structures. Lorenz, et al. (2003) indicates that large periods of right-lateral strike slip movement dominated the deformation of the northeastern and northwestern structures surrounding the basin.

The three phases are distinctly separated by basin-wide unconformities. The first phase of sedimentation due to subsidence is responsible for the Fruitland and Kirtland Formations and it occurred about 74-67 Ma during the late Campanian and early Maastrichtian periods (Cather, 2003). The second phase is characterized by the Ojo Alamo and Nacimiento sandstones, and it occurred about 67-61 Ma during the late Maastrichtian and early late Paleocene periods (Cather, 2003). The final phase is represented by the San Jose Formation, and it occurred during the middle Eocene and early Oligocene periods. Although the San Jose Formation is all that remains from the third phase, data suggests up to one kilometer of sediment was deposited and subsequently stripped away from the San Juan Basin (Cather, 2003).

The relationships between units and their borders, delineated by the uplifting, is indicative of syntectonic basin filling (Cather, 2003). This is where the angular unconformities are observed. One place where it can be observed in outcrop is at the contact between the

McDermott and the Animas Formations in the dipping limb of the Hogback monocline southwest of Durango, CO.

Hogback Monocline

Similar to other monoclines of the Colorado Plateau, the folding of the Hogback Monocline began during the Paleozoic and was completed by the early Eocene (Kelley, 1955; Lorenz et al., 2003). The Hogback Monocline delineates the northwestern portion of the San Juan Basin (Cather, 2003). Although the structures seem continuous from the Hogback Monocline to the Archuleta Anticlinorium there is a distinction made between the two. Both their general orientations and the differences in their overlying sediment packages are enough to make a clear distinction (Cather, 2003).

The general trend of the Hogback Monocline is northeast-southwest and it stretches approximately 60 miles. In many places, the geometry of the monocline's dipping limb wavelength and axial trend changes. Lorenz et al. (2003) describe these changes as being structurally and geometrically related to Ute dome and Barker dome, and interpret this relationship to indicate right lateral

Figure 4: Arial image showing topographic expression of the Hogback Monocline. Similar monocline orientations are shown in the same colors to increase visibility of bends.

wrench faulting at depth along an en echelon basement geometry. Some of these changes in geometry along the length create the bends of interest. There are four distinct bends that demonstrate the S and Z bend nature observed in the topographic expression of the monocline (*Figure 4*).

Currently, near Waterflow, NM, the topmost unit is the Fruitland Formation. Moving down section, to the northwest side of the monocline, the Mancos Shale is exposed. The ridgeline consists of the Mesa Verde group, which includes the Cliff House Sandstone, which was our primary study area.

Several of the Hogback Monocline fracture sets have been described. The earliest set, interpreted by Condon (1988; 1997), strikes average north-northwest south-southeast, changing with respect to both structural and stratigraphic position (Lorenz et al., 2003). The oldest set strikes average north-northeast south-southwest, and are normal extensional fractures (Lorenz et al., 2003). Erslev (2009) points out that the fractures associated with the Hogback Monocline do not match fractures seen within the basin, and their relationship is unknown.

Modeling

Over the past 100 years, the investigation of structures in the Rocky Mountain foreland has resulted in numerous structural models involving basement structures (Mitra & Mount, 1998). The point of much of this modeling is to understand the geometry of the basement faults and their geometric relationship to the deformed stratigraphy in the monoclines. The primary focus of many of these studies is the mechanical origin and mechanisms associated with the deformation of these structures. Creating experimental models involves scaling these features down to study the evolution of these structures. These structural models are based on surface

observations and are used to investigate the subsurface, where data is lacking. The geometric relations of reverse, normal, and vertical displacement, and the overlying stratigraphy is becoming better understood through the use of these models. It is understood that real structures are complex, and models cannot recreate all observed features, but they can be applied to case studies to make general predictions of subsurface geometries of features. While the predictions may be generalized, these models can make a wide variety of interpretations regarding foreland basement structures (Mitra & Mount, 1998; Reches, 1978).

Creating robust predictive models requires a consistent framework and judicious choice of parameter values (Dee et al., 2007). An advancing area of modeling is the use of geomechanical modeling to create discrete fracture network models (Dee et al., 2007). These require an understanding of the mechanical properties and paleoregional background strains (Dee et al., 2007). Another area of modeling consists of geometric and kinematic modeling, which are used to investigate the evolution of the structure as a whole (Mitra & Mount, 1998). Mitra and Mount emphasize the importance of considering rock mechanical property variations in the models, but Dee et al. (2007) notes that this importance really affects fracture criterion. The kinematic and geometric models investigate the transfer of slip on the basement fault to the folding associated with it in the overlaying cover. Described by Mitra and Mount (1998), there are three kinematic model types used to investigate these structures, and they are: (1) the drape fold or force fold model, (2) the upthrust model, and (3) the thrust geometries model.

For the fault models to generate realistic results, the fault must be modeled at the depth it had during the slip event, this is especially important during the generation of elastic dislocation models (Dee et al., 2007). Another area important to consider is the mechanical process

occurring during low temperature deformation, such as flexural slip and a number of brittle and ductile mechanisms, resulting from mechanical stratigraphy (Mitra & Mount, 2007).

Modeling has led to a vast amount of resulting data and understanding of geologic structures. A significant result for the understanding of monoclines of the Colorado Plateau is that a very small amount of horizontal shortening can produce significant amounts of relief in structure, when the movement is along a steeply dipping fault (Davis, 1978). Although there is a large amount of consensus that these structures are related to high angle reverse faults, it is necessary to further determine the dips of the master faults (Miller & Mitra, 2011). In the modeling, a consistent result is that the basement fault breaks through the overlying stratigraphy when the throw overcomes one-third to one-half the thickness of the stratigraphic package above it (Mitra & Mount, 1998). The angle of the underlying fault is thought to have a large role on the width of the deformation zone, where steeper dipping faults have narrower deformation zones above them than shallower dipping faults (Miller & Mitra, 2011). In compressional environments, there are secondary reverse faults that form and lead to significant amounts of deformation in the triangular deformation zone (Erslev, 2009; Miller & Mitra, 2011). The orientations of the bounding axial surfaces, and the distributions of secondary faults, provide evidence for the dip of the underlying fault (Miller & Mitra, 2011). Dee et al. (2007) suggests that the secondary faulting occurs as stress perturbations during coseismic slip. In relation to the dip of the fault, Mitra and Mount (1998) indicate that strike-slip faulting may play a role in a number of these structures.

Methods

The methodological goals of this investigation were to move from conceptual models, shown in *Figure 5,* to numerical models, and then compare the results of these models to a case study. There were three conceptual models we used to approach this problem, each of which utilize a different basement fault geometry. Each conceptual model was then used to develop 3D elastic dislocation models. The results of these models were then compared to field data to demonstrate their accuracy, and show how they can be used to predict subsurface geometries of structures.

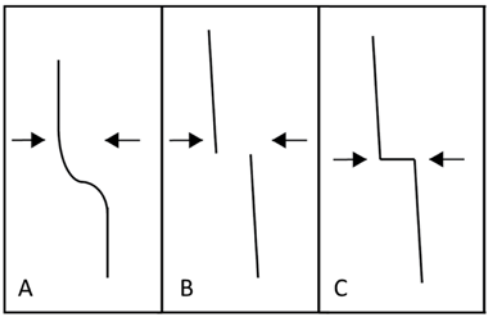

Figure 5: Conceptual models in plan view of fault geometries. (A) Singular fault following topographic expression of the bend in the monocline. (B) Simple relay model. (C) Breached relay model.

Field Work

The primary influence on designating the field area was the accessibility and availability of outcrop of the dipping limb of the monocline, in a place where the monocline demonstrates the desired bend of the axis. On the Colorado Plateau there are many places where monoclines have bends in their axes, but few fit the scope of this project. The section of the Hogback Monocline stretching north of Highway 64 near Waterflow, NM contains bends of interest with near continuous exposure. There are four bends of interest between Waterflow, NM and

Durango, CO, including the one that has been designated as the field area for this investigation (*Figure 6*).

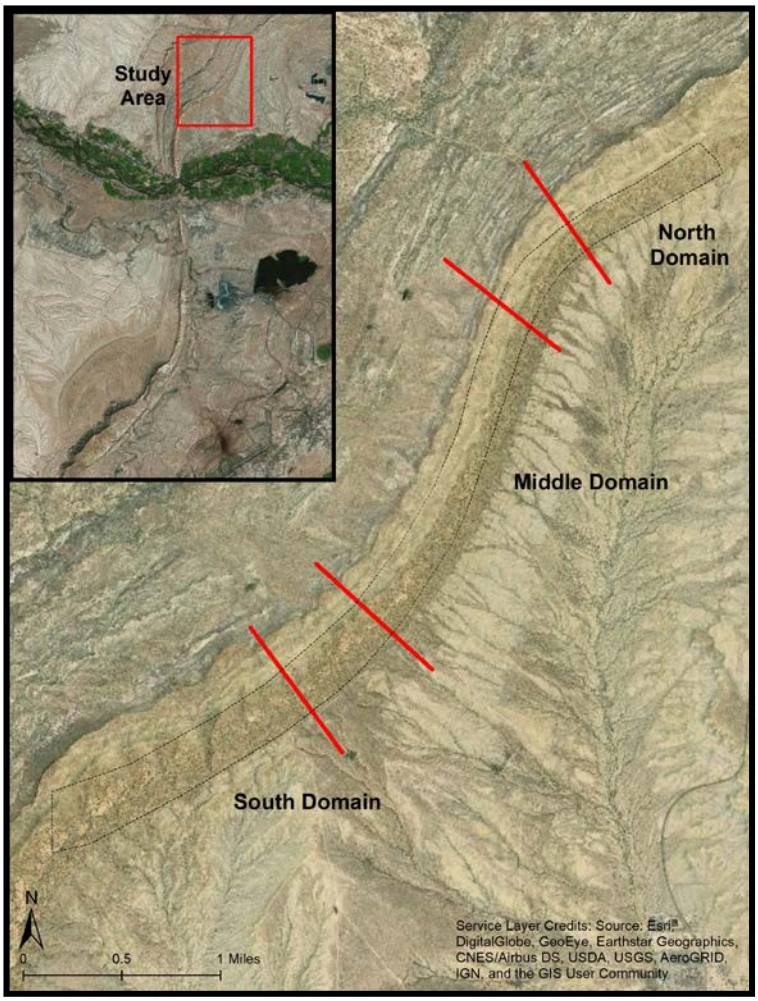

Figure 6: Map of field area. Field area lies three miles north of Highway 94 along the Hogback Monocline. Indicates selected domains along the study area. Red lines indicate breaks between domains of data used for comparison to models.

Significant differences in mechanical properties can originate from differences in original and diagenetic compositions (Erslev, 2009; Lorenz et al., 2003). In order to control for variation in rock strength with lithology, and due to time limitations, the measurement area was limited to

a narrow curvilinear area that stays consistently within the same units in the Cliff House Sandstone.

Field Data Collection

The fracture data was collected with Brunton Compasses and Garmin GPSs. Strike and dip measurements were collected at each point as well as trend, plunge, and rake when slicken lines where present in the fractures.

In the initial field observations, it became apparent that there are at least four distinct sets of fractures. The aim of the measurement process was to collect similar numbers of measurements per set to maintain consistency for statistical power.

Data Analysis

For the data analysis and interpretation, StraboSpot and stereonets were used. StraboSpot was used initially for data visualization and organization. StraboSpot is an online database designed to allow structure and tectonics data to be systematized and shared (https://www.strabospot.org/overview). The strikes, dips, latitudes, and longitudes of the fractures were uploaded into StraboSpot to assist with the categorization of the spatial distribution of the fracture orientations. Because all four of the fracture sets extend the entire length of the monocline, they were uploaded to StraboSpot as individual datasets. The fracture orientations were categorized into five sections. The sections are delineated into straight domains and bent sections. There are three straight domains broken up by the two bent sections (*Figure 6*). Once the sections had been delineated, stereonets were used to plot the data of each of the straight domains to compare to that of the straight domains of each of the models.

Data Cleaning

In the stereonet software, dip directions were corrected and outlier planes were removed. Data planes were removed from the datasets on the basis that they fell into another dataset. Each dataset contained sufficient data to maintain statistical power while removing inaccurately classified data. When data points were removed, it was assumed that they belonged to other datasets, and therefore were already accounted for in the study.

In some instances, the fracture classification was mistaken in the field, and in stereonet there were outlier fracture planes that did not fit within the fracture set. The strike-parallel fractures were corrected to dip to the west when they were dipping to the east. It was apparent in the field that all of the strike-parallel fractures dip to the west and northwest, and none to the east.

During field data collection, there was a period when the Fort Lewis College undergraduate Structural Geology class assisted in data collection. Although this class has gone through the Geologic Field Methods class, significant practice with the Brunton Compass is still lacking. In these cases, the fractures that clearly did not fit within one the known fracture set were removed.

The strike-parallel fractures and bedding datasets were the ones of greatest interest and therefore were given the most attention during data cleaning. The reason for this was that during the T7 modeling we learned that our models can quantify bedding orientation and reproduce only the strike-parallel fracture orientations.

T7 Modeling

The modeling software used in this investigation was T7 by Badley Geoscience. In T7, the T7 fracture module uses an elastic dislocation method that relates slip on faults to stress and strain in the surrounding rock volume via linear elastic mechanics. In the models we used pre-determined faults and slip to deform an initially horizontal observation grid representative of the Cliff House Sandstone. T7 solves for the principal stress magnitudes and orientations at each node on the grid. If stress conditions exceed the rock strength, T7 predicts a fracture, with the type and orientation determined by the local stress. T7 uses a corner point grid to calculate the stresses and strains that result from movement on a fault, or from imposed strains on the boundaries of the model. Stresses are calculated assuming elastic behavior of the rocks, and brittle failure is predicted using Mohr-Coulomb failure analysis. This type of modeling is a geomechanical, elastic dislocation modeling system, which has been used extensively for the generation of discrete fracture networks associated with large faults and further modeling based on these networks (Dee et al., 2007).

The parameters investigated in T7 for the forward models were: fault slip directions, throw amount, percent strain applied at the volume boundaries, and rock mechanical properties. Dee et al. (2007) indicates the importance of a judicious selection of property values, and because of this we based our parameter values off previous published values. Some of these parameters were used as variables while others were set as constants. The throw amount and rock mechanical properties were set as constants for the models. The throw was obtained by comparing the structural relief across the monocline at the surface. The rock mechanical properties were generalized to match that of sandstone. By setting the rock properties of the volume to match that of sandstone, the models simulate the strain experienced by a homogenous

volume like in Dee et al. (2007), although Stearns (1978) and Mitra & Mount (1998) emphasize the importance of mechanical stratigraphy. As is common in modeling, the rock mechanical property values used were from previous literature and the T7 manual (Ahrens, 1955; Dee et al., 2007) and consisted of angle of internal friction (0.6), Young's Modules (20,000 MPa), and Poisson's ratio (.25).

The three fault systems were created in the T7 model volume (*Figure 7*) using the topographic expression of the study area on the Hogback Monocline. All three of the fault geometries consist of two fault segments that run parallel to each other and are offset by 1400 meters. The first model consists of one fault with an S-bend. The second fault model geometry consists of three faults and is known as a breached relay fault system. The third consists of only two faults and is known as a simple relay fault system. The S-bend fault geometry and simple relay are the two endmembers of the conceptual models investigated. Due to time limitations and Mitra & Mount's (1998) focus on the endmembers of their systems of interest, we also only investigated the two endmembers.

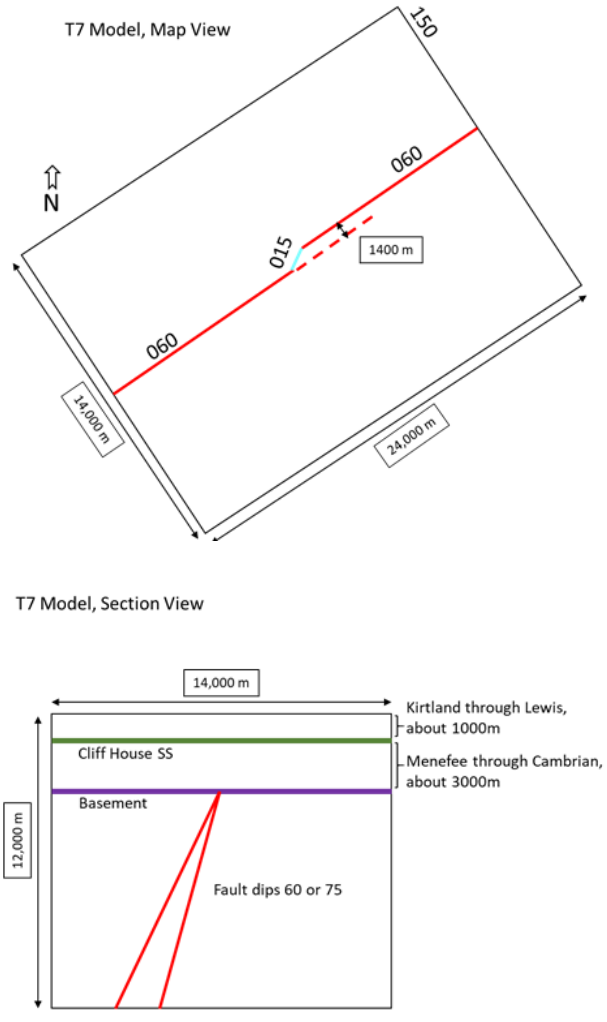

Figure 7: T7 model volume dimensions. The plan view dimensions follow topographic expression and the cross sectional dimensions were derived to recreate paleo burial stresses during deformation.

As suggested by Dee et al. (2007), the tops of the faults were placed at a paleodepth, in our field area this was estimated to be 4000 meters. This depth is at the contact between the basement and the overlying stratigraphy, such as the models created by Mitra & Mount (1998). In the models, all three of the fault geometries are striking 60º east of north. The volume of the models is 4032 m^3 with dimensions of 14 x 24 x 12 km. The stresses imposed on the volume resemble compressional stresses that lead to the general formation of monoclines *Figure 8*, in which σ1 is horizontal and σ3 is horizontal, where σ1 > σ2 > σ3. This differs from Miller and Mitra's (2011) stress regime, where σ3 is vertical instead of horizontal. Imposing a horizontal σ3 predicts vertical fracture, where as a vertical σ3 predicts horizontal fractures. Based on observed vertical fractures in the field the model needed a stress regime that could account for the vertical fractures.

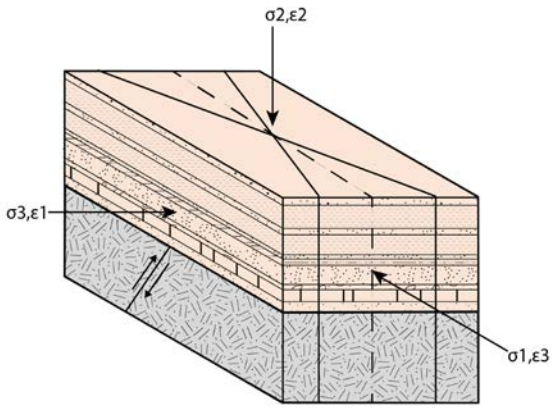

Figure 8: Stress regime imposed on block model. The model shows a faulted basement as well as predicted fracture orientations associated with this stress regime.

Beyond the three fault system geometries and the model parameters, another variable accounted for was the dip of the faults, because there is no direct data on the dip of the fault underlying the Hogback Monocline. For each fault geometry two fault dips were used, and they were 60º and 75º based on values described by Miller & Mitra (2011). Although dips of 30º–60º

are typically used for compressional structures (Miller & Mitra, 2011), in this investigation dips of 60^{o} and 75^{o} were used because the Hogback Monocline has been interpreted as a structure with a reactivated Neoproterozoic extensional fault system (Cather, 2003; Davis, 1978; Davis & Bump, 2009; Twiss & Moore, 1992).

In the model volume, a rasterized observation grid was placed at the estimated paleodepth (1000 m) of the Cliff House Formation (*Figure 7)* with a resolution of 10 meters. By placing the grid at this depth, the resulting data are representative of Cliff House Sandstone immediately following deformation while still experiencing the stresses associated with burial depths. The grid shows the shape of the monocline (uplift, wavelength, limb dip, and bend geometry), stress and strain parameters on the grid (suggesting how the intensity of fracture development varies), principal stress and strain orientations, and predicted fracture types and orientations.

These results were used during the initial qualitative analyses to determine which models produce results that were not realistic and results that were realistic enough to need more analysis. Although the observation grid was used to show multiple types of results, the primary results used thus far were fracture prediction orientations and resultant dips of bedding along the dipping limb of the monocline. The results of the models were compared to the field observations and measurements in order to assess their validity. When fracture orientations showed similar patterns to the field orientations, they were determined to be valid. Bedding orientation was also assessed on the basis of qualitative geometry, as well as quantitative geometry.

It is understood that the models are simplifications of reality, and therefore cannot depict all details observed in the field, nor are they exactly deterministic in predicting subsurface

geometry (Mitra & Mount, 1998). The models recreate the strike-parallel fracture orientation only, and by doing so only tell part of the deformational story.

Out of the realistic resulting models, the fracture orientations were exported in domains, as text files, to match the delineated domains of the field. The text files were then imported into stereonet for quantitative and further qualitative analyses.

Changes in local and regional stress strain relationships differ between the basement and the overlying stratigraphy (Maerten et al., 2002; Dee et al., 2007). The deformation experienced by the stratigraphy is a reflection of the strain experienced by the rigid basement and ultimately generated from plate tectonic stresses (Davis & Bump, 2009). Because of these differences, parameters that were used to investigate the difference in stress between the basement and cover stratigraphy were fault forced movement and imposed boundary strain that lead to the desired 900 meters of throw. In the fault force parameter models, the stresses created are from the movement of the fault, and therefore reflect local strain from the formation of the monocline. In the models with boundary strain conditions imposed, the strains experienced are regional instead of local (Davis & Bump, 2009).

Results

Field Observations

There are several different orientations and types of fractures present. The clear majority of the fractures are joints. We have grouped the fractures in three sets: strike-parallel, dip-parallel, and oblique to both strike and dip and plotted them into domain specific stereeonets for the extent of the field, which are shown in *Figure 9*.

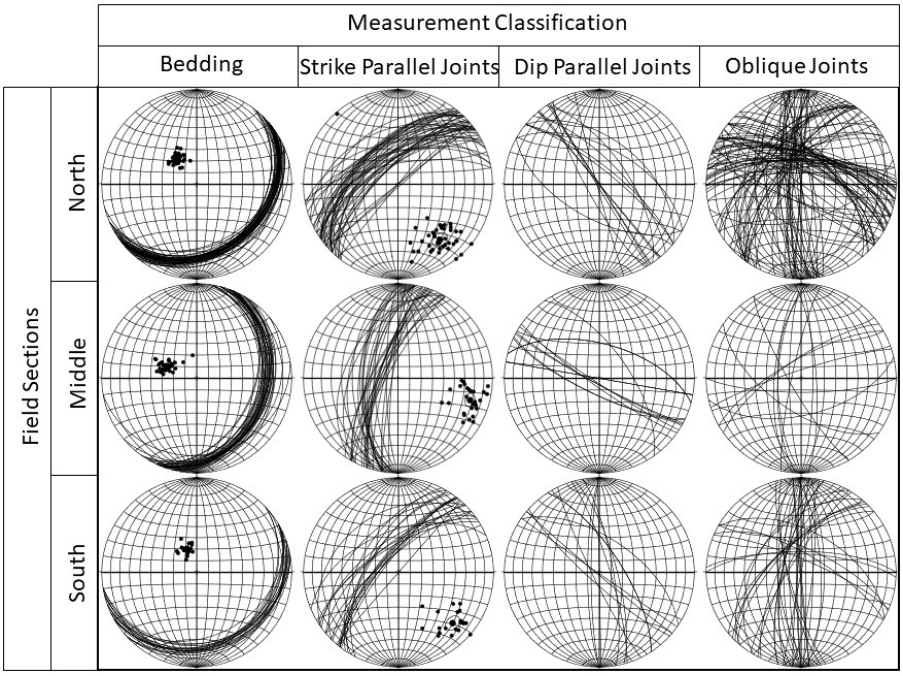

Figure 9: Compilation of field data in stereonets. The data is organized into orientations of bedding, strike-parallel fractures, dip-parallel fractures, and oblique fractures, and are also separated by domains.

The oblique joints have several different orientations, however the dominant two seem to demonstrate a similar geometry to conjugate shear fractures. However, evidence of shear is lacking in the majority of the field area, possibly due to weathering as caliche is present on many of these fracture surfaces. Three fault surfaces were found that have horizontal slicken lines

present; on these surfaces slicken lines are laterally discontinuous, showing signs of weathering (*Figure 10*). While others may be present, the few we have found are not enough to make confident analyses from.

Figure 10: A weathered fault surface showing slicken lines. The dark grey line delineates the weathered surface from the surface that shows slicken lines. The slicken line orientation is shown by the black lines, whereas the bedding is shown by the light grey lines.

Along the outcrop of the Hogback Monocline, or rather the Hogback Ridgeline, the Mesa Verde group makes up the lithology of the ridgeline. The primary study area was located within the Cliff House Sandstone, which here consists of interbedded shale and sandstone (*Figure 6)*. In some areas there are isolated changes in the cementation that create small pods within the same beds moving laterally. These red cement pods are dense and have much higher levels of fracture intensity and become more chaotic (*Figure 11)*, but outside of these pods, the Cliff House Sandstone is relatively consistent. Thus, the fracture measurements are coming from a consistent rock. As a means to maintain consistency in measurements, not much attention was given to

these pods, other than noting their presence, and no evidence of mechanism of creation was apparent. In other areas, joints show evidence of fluid movement and contain a cement of an iron mineral interpreted to be hematite.

Figure 11: Images of increased cemented pods. On the left, increased fracture intensity as well as the increased chaos in fracture orientation is shown. On the right, the photo shows how these pods are laterally discontinuous.

Moving north to south on the ridgeline from the straight portions of the monocline to the bent portions, the strike and dip of the bedding change noticeably. The strike of the bedding within the north and south sections is almost parallel, and the middle domain is rotated counter-clockwise from that of the other two sections.

The orientations of fractures with respect to the cardinal directions and the bedding also exhibit noticeable changes (*Figure 9)*. Fracture orientation changes with respect to both the stratigraphic and structural position in the monocline. Between the north, middle, and south domains of the monocline (*Figure 6)*, the strike of the strike-parallel fractures changes in orientation (*Figure 9)*. The strike-parallel fractures demonstrate similar orientations to the strike of the bedding. The north and south domains exhibit fracture strikes that are very similar, and the

middle domain has a strike rotated counter-clockwise in relation to the other two domains (*Figure 9)*.

Similar to both bedding and strike-parallel fractures, the dip-parallel and oblique fracture sets change orientation along the trend of the monocline (*Figure 9)*. The change in orientation of the fracture sets is dominantly the change of strike. The dips of the fractures are consistently between 50-80 degrees. While their dips vary by about 30 degrees, the change of strike along the monocline is consistently dependent on domain, whereas the variation in dip of the fractures seems to be more chaotic. The strike of the dip-parallel fractures also rotate counter-clockwise in the middle section, like the strike of bedding and of the strike-parallel fractures. Although the oblique fracture sets show much more variance than the other two sets, they follow suit and show counter-clockwise rotation in the middle domain of the field area.

Moving between layers, the dominant fracture set varies. While strike-parallel fractures and oblique fractures may be dominant in one layer, a layer overlying or underlying it may solely exhibit dip-parallel fractures. However, dip-parallel fractures are the least common fracture set present across domains in our observations. Moving laterally, across domain boundaries, fracture type dominance changes as well. While there may be a change in fracture density of orientations, all fracture orientations are present along the study area. Although all fracture sets are present along the full length, their orientations change azimuth, but their orientations to bedding remain consistent.

The crosscutting relationships exhibited by the fracture sets are inconsistent along the length of the study area. However, within subsets of each domain, the crosscutting relationships seem to be similar. For example, in the northern section, strike-parallel fractures are semi-

continuous while breaking the oblique fracture sets, and in other areas different sets are broken instead (*Figure 12*).

Figure 12: Outcrop photos showing crosscutting relationships of fractures. On the left, there are semi-continuous strike-parallel fractures cutting oblique sets of fractures. On the right, there are strike-parallel fractures cutting dip-parallel fractures. The left photo was taken in the north domain and the right photo was taken in the middle domain.

T7 Modeling

Although the T7 modeling produced many quantitative results, we only had time to interpret a few of them, but there is a significant amount of promise in the results that were produced. The primary result of interest is the creation of a monocline with an S-bend present (*Figure 13*). Each fault geometry was able to produce a similar S-bend geometry in the monocline as seen in outcrop. Although the S-bend is produced by the modeling, the wavelength is too broad and the dipping limbs' dip are not steep enough to be representative of what is seen in outcrop.

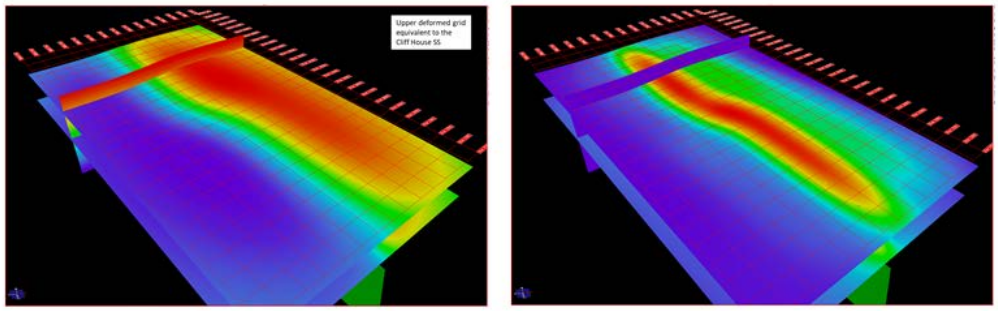

Figure 13: Observation grid showing S-bend monocline geometry with both elevational results and differential stress. On the left is the resulting elevation, blue represents subsidence and red represents uplift. On the right is the differential stress result, with blue representing lower differential stress and red representing higher differential stress, this image shows the highest stress in the region of the dipping limb.

The real beneficial outcomes of the modeling in this project are methodological. The primary results that were analyzed were fracture orientations in the horizontal observation grid. Domain fracture sets were exported and plotted in a stereonet, shown in *Figure 14*.

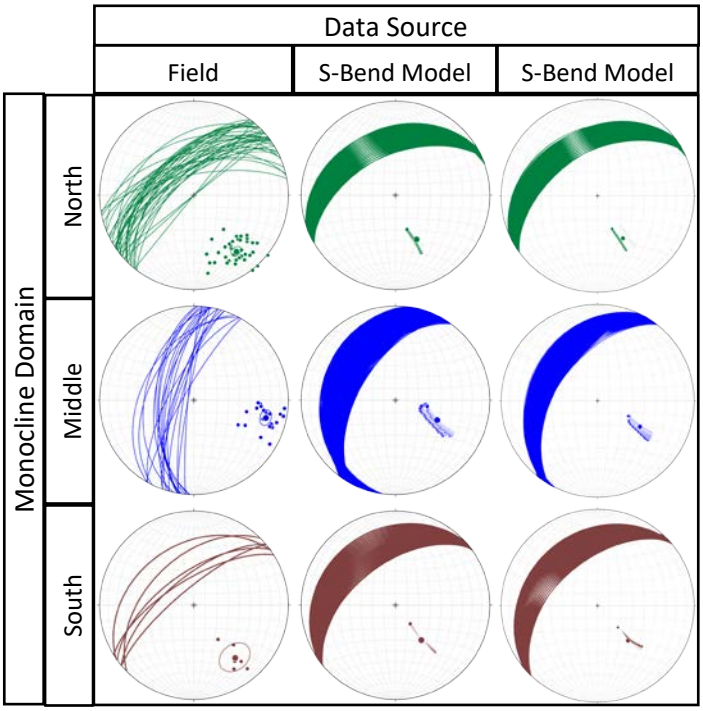

Figure 14: Field and modeled fracture orientations in stereonets. Here the data is categorized by domains of strike-parallel fractures from the field and the fractures predicted by the S-bend model and simple relay model.

Amongst the variation in the slip direction and strain boundary condition parameters, dip slip movement of the fault produce fracture orientations that reflect what is seen in the field, along the dipping limb of the monocline.

Both end member models predict fracture orientations similar to the fracture patterns seen in the field *(Figure 14)*.

The models only produce one set of fractures along the observation grid of the monocline. The set that they produce is the strike-parallel fracture set, all of which are predicted to be tensile fractures. The models do predict other types of fractures and orientations but in other positions in the structure (*Figure 15*). The dips of the strike-parallel fractures predicted in the models are 20^{o} less, on average, than that of the dips seen in the field. While our models reproduce similar orientations of strike parallel fractures, it is important to acknowledge the importance of slip direction on their resulting orientations. Any oblique slip changes the orientation of the strike-parallel fractures away from what is observed in the field.

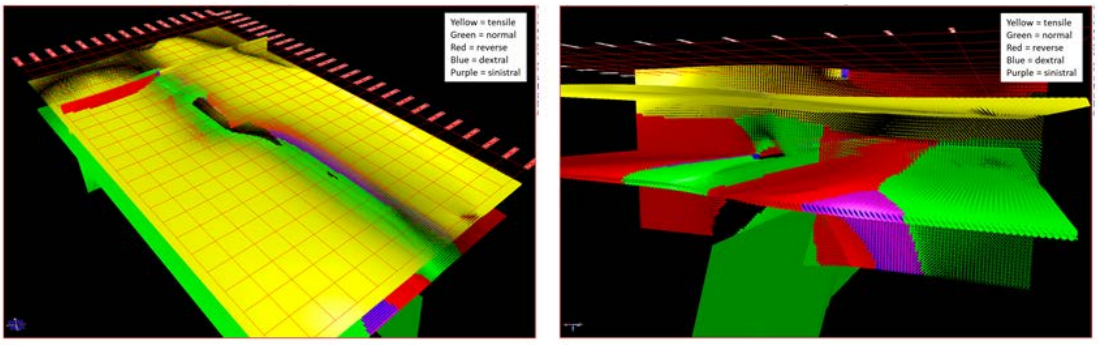

Figure 15: Resulting T7 fracture predictions for S-bend model. Colors represent fracture types as follows: Yellow = tensile; Green = normal; Red = reverse; Blue = dextral; Purple = sinistral.

Discussion

Field Data

The fractures along the monocline change in orientation depending on position in the structure, the fracture sets indicate a change in local stress orientation. Looking at the strike-parallel fractures of all three domains, the counter-clockwise rotation of the middle domain's mean strike indicates a change in stress orientation. This is due to the fact that tensile fractures occur perpendicular to the extensional stress applied on the medium and/or the folded layer.

The presence of multiple sets of fracture orientations indicates several deformational events. At least one to two deformational events must have taken place during the time of Laramide deformation because there are three distinct sets of fractures and two sets that may or may not be genetically related. The strike-parallel and the dip-parallel fracture sets are indicative of two separate events, or rather stress regimes. While the separate oblique fracture sets resemble conjugate shear fractures and are kinematically compatible with the dip-parallel joints, the two types of fractures require different stress ratios. Although the angles between these two fractures' orientations resemble conjugate shear fractures, there is not enough evidence of movement along these fractures to classify them as such. The majority of fracture surfaces are weathered or coated in caliche (*Figure 10*), making a clear interpretation difficult. There are a few surfaces that share the same orientation as the oblique fractures with horizontal slicken lines present. These few fracture surfaces with slicken lines may have experienced less weathering than the other surfaces observed, but at this point making a classification is not possible.

There are many descriptions of periods during the Laramide where the stresses experienced by the San Juan Basin's perimeters – specifically the northwestern and northeastern

perimeters – caused strike slip movement. The orientations of the oblique fracture sets do not seem to fit the strike slip kinematics described by literature. If the acute angle between the fractures was oriented northeast-southwest, then this interpretation would work, but the acute angle is oriented northwest-southeast, and therefore resembles dip slip oriented strain. One of the pieces of evidence used to support strike slip movement is an en echelon (stair-step) geometry seen in the topographic expression of the structure. Although en echelon geometries are consistent with shearing caused by strike slip environments, they can also occur from extensional conditions. Based on the assumption that these structures have formed from the reactivation of Neoproterozoic faults, they were formed during an extensional environment, and their geometries were predetermined before Laramide deformation began. So even if strike slip movement occurred, the en echelon pattern is not a result of this movement.

Laying perpendicular to the strike-parallel fractures, the dip-parallel fractures are also tensile fractures. There seems to be no evidence of slip along these surfaces. These fractures align themselves with the fractures predicted by the conceptual model where $\sigma 1$ is horizontal and $\sigma 3$ is horizontal, where $\sigma 1 > \sigma 2 > \sigma 3$. Although this differs from the general stress regime indicated by Miller & Mitra (2011), it accounts for vertical fractures while still implying a compressional environment. Tensile fractures occur perpendicular to $\sigma 3$ and this is how this stress regime accounts for vertical fractures.

The stress regime where $\sigma 1$ is horizontal and $\sigma 3$ is horizontal reflects regional stress regimes much more than the local stress regime of the folding of the monocline. Both local and regional stress regimes are accounted for while interpreting fracture sets, assuming the strike-parallel fractures are a response to local stresses, while the dip-parallel and oblique fractures reflect regional stress regimes. In making this assumption, the oblique fracture sets must be

conjugate shear fractures. While the evidence in the field is not sufficient to quantify this, the overall evidence between the field fracture orientations, literature, and our models suggest that these are conjugate shear fractures. The field evidence that supports the conjugate shear fracture orientation is that the acute angle is more closely aligned with σ1 than any other stress direction, which is how the stress regime described by Miller & Mitra (2011) is oriented. In addition to the acute angle being aligned with σ1, it is also aligned with the dip-parallel fractures, as predicted by the vertical fracture stress regime model. This orientation of σ1 is interpreted to be associated with late Campanian and early Maastrichtian time, approximately 74-67 Ma (Erslev, 1997).

As discussed in the results, there is a variation of fracture cross-cutting relationships across structural and stratigraphic position on the Hogback Monocline. These changes in cross-cutting relationships indicate different parts of the monocline experienced different stresses simultaneously. This is in agreement with Davis (1978), who indicated that there was differential strain within a single structure.

Modeling

While approaching the modeling in this project, the hypothesis was that the fault geometry would affect the discrete fracture network orientations to such a degree that one would provide predominantly more realistic results. However, at this point the largest factor in fracture orientation was slip direction. Mitra and Mount (1998) as well as Lorenz et al. (2007) suggest that there were periods of strike slip wrench faulting at depth beneath the Hogback Monocline. However, the modeling suggests that only dip slip movement can create the strike-parallel fractures seen in the field.

Changes between local and regional stress-strain relationships lead to creating conditions where the resulting modeled data is only useful on and in the direct vicinity of the modeled monocline (Fig. X). The parameters that create a model with realistic resulting monoclines also predict unrealistic fracture orientation towards the boundaries of the model. Although the modeling lacks validity through the entire volume, it is credible where we have field data to compare.

Similarly, it is important to remember that models do not recreate all observed features, and it is important to assess the model's validity based on more than one of its results. For instance, the fracture orientations created by both models resemble that of the outcrop fractures. Yet the resulting bedding geometries of the dipping limbs of the models dip about 20^{o} less than on the Hogback Monocline. We have interpreted this change in dip to be possibly related to the depth of the fault, as well as the dip of the fault.

Conclusions

Towards the beginning of the project the hypothesis was that the individual basement fault geometries would yield results indicating a preferred basement geometry based on the discrete fracture networks predicted by the models. When all of the models were able to produce predictions with similar orientation patterns, it became clear that there are more intricacies involved with the setting of the model parameters. Both the S-bend model and the simple relay model produce S-bend monoclinal geometries, indicating that our conceptual model hypotheses have validity. Although the monocline geometry of the S-bend is reproduced, the wavelength of the monoclines are inaccurate and do not reflect what is present in the field.

Affecting the patterns of fracture orientations more than the fault geometry is the slip direction. Although previously published literature suggests strike slip to oblique slip movement, our models' results indicate that the fractures seen in outcrop are not the result of this right lateral slip. In addition to the models' fracture orientations indicating slip direction, the kinematic relationship between the oblique fractures and dip-parallel fractures are strong evidence for dip slip movement. In turn, all of our data suggests dip slip movement, which directly contradicts previously published works that indicate strike slip movement was a factor in the formation of the Hogback Monocline.

As is indicated by many authors, the importance of improving the understanding of the timing of fracture formation and their orientations within these structures plays a big role in industry advancement. While this project aimed to interpret the preferred geometry of basement faulting from 3D numerical modeling, compared to a case study, to improve the predictability of discrete

fracture networks in the structure, it also led to developing preferred stress regimes and kinematics. While a preferred fault geometry is still unknown, the understanding of the role which various parameters have on the results improves the understanding of the Hogback Monocline in ways we did not predict.

Future Directions

Additional T7 Modeling and Analysis

Due to the time limitations leading to the investigation of only the end members of the conceptual models, this research would greatly benefit from more numerical modeling. In addition to more modeling, the models that have already been run still require more analyses to improve the parameter selection for the new models. Although the fracture strikes of the models reflect the general orientations seen in outcrop, their dips are up to 15^{o} less steep. Similarly, the bedding dips average about 20^{o} less steep than in the outcrop. These are two results worth attempting to improve before moving on in the modeling process. The wavelength of the monocline is another factor that deserves move investigation, both in the field and T7 models. In addition to modeling in T7, it would be beneficial to approach the modeling while acknowledging the different mechanical properties present in the basement and all of the stratigraphic units. As well as acknowledging rock properties, a model that accounts for several deformational events would greatly benefit this process, due to the fact that there is evidence of multiple generations of deformation, yet T7 can only account for one. A modeling method that can acknowledge both rock properties and multiple generations of deformation, is finite element modeling.

Field Kinematics

The use of field kinematics could better improve the understanding of the strain directions experienced by the Hogback Monocline and thereby improve the modeling parameters and the validity of the models, while narrowing the list of unknowns. In the outcrop, deformation

bands may not be everywhere, but there are still prevalent. Less commonly found in the field area are slicken lines on fault surfaces, but these also are an ideal form of field kinematics. For clarification, field kinematics is used here in the context of field evidence indicating movement, more specifically directional movement within the structure.

Clay Modeling

As an analog to the work that has been done thus far in the field and with T7, clay modeling would benefit this project vastly. The culmination of digital modeling with analog modeling and a case study would bring the addition of credibility to this work. The clay modeling should use the T7 modeling as a basis instead of starting from scratch. By doing so, each of the conceptual fault geometry models should be investigated. In addition to using the conceptual fault model geometries, the parameters in the clay models can also benefit from the work already done in T7 that has determined the importance or change in results based off of these parameters. The benefit of the clay model is having a real world check on the numerical modeling done in T7.

Acknowledgements

The field investigation was made possible by the Mineral Department of The Navajo Nation. Without granted access this project would not have been possible. A great thank you to Badley Geoscience for providing the T7 Software and technical support when needed. Thank you to Kim Hannula and Bob Kranzt for making this project possible, and the devoted support. To Kim your encouragement and unwaving support made it possible for me to finish this thesis

and there by possible to graduate. To Bob your vast knowledge base in this field and your understanding of the troubles that come with the modeling process made the process less painful and much more enjoyable. Without the assistance of my partners, in the project, Eric Wzientek and Cameron Gaco the extent of field data collection and modeling would not have been possible and the results would have been for fewer. Thank you to the Structural Geology class of the fall of 2018 for spending an entire day out in the field collecting fracture orientation data, giving the data a statistical power that would have been possible otherwise. Thank you to Alena Egnar for acting as my scribe and making it possible for me to produce and finish my thesis at the level that it reached. Lastly thank you to my parents Jay and Christina Lancaster for making all of this a possibility and through my hard work and their support a reality for me.

References

Ahrens, T.J., 1995. Mineral physics & crystallography: a handbook of physical constants (Vol. 2). American Geophysical Union.

Anderson, H., Davis, G. H., and Davis, T. J. 2015. 3-D structural modelling of the East Kaibab Monocline in northern Arizona: Abstracts: Annual Meeting - American Association of Petroleum Geologists, v. 2015.

Brandenburg, J. P., Alpak, F. O., Solum, J. G., and Naruk, S. J., 2012. A kinematic trishear model to predict deformation bands in a fault-propagation fold, East Kaibab Monocline, Utah: AAPG Bulletin, v. 96, no. 1, p. 109-132.

Cather, S. M., 2003. Polyphase Laramide tectonism and sedimentation in the San Juan Basin, New Mexico: Guidebook - New Mexico Geological Society, v. 54, p. 119-132.

Davis, G. H., 1978. Monocline fold pattern of the Colorado Plateau: Memoir - Geological Society of America, no. 151, p. 215-233.

Davis, G. H., and Bump, A. P., 2009. Structural geologic evolution of the Colorado Plateau: Memoir - Geological Society of America, v. 204, p. 99-124.

Dee, S. J., Yielding, G., Freeman, B., Healy, D., Kusznir, N. J., Grant, N., and Ellis, P., 2007. Elastic dislocation modelling for prediction of small-scale fault and fracture network characteristics: Geological Society Special Publications, v. 270, p. 139-155.

Erslev, E., 2009, Integrated fracture analysis: An important tool for deciphering complex fracture patterns, in Proceedings, Adapted from oral presentation at AAPG Convention, Denver, Colorado, June 7-10

Kelley, V. C., 1955. Monoclines of the Colorado Plateau: Bulletin of the Geological Society of America, v. 66, no. 7, p. 789-803.

Lorenz, J. C., and Cooper, S. P., 2003. Tectonic setting and characteristics of natural fractures in Mesaverde and Dakota reservoirs of the San Juan Basin: New Mexico Geology, v. 25, no. 1, p. 3-14.

Maerten, L., Gillespie, P. and Pollard, D.D., 2002. Effects of local stress perturbation on secondary fault development. Journal of Structural Geology, v. 24 no. 1, p.145-153.

Miller, J. F., and Mitra, S., 2011. Deformation and secondary faulting associated with basement-involved compressional and extensional structures: AAPG Bulletin, v. 95, no. 4, p. 675-689.

Mitra, S., and Mount, V. S., 1998. Foreland basement-involved structures: AAPG Bulletin, v. 82, no. 1, p. 70-109.

Reches, Z., 1978. Development of monoclines; Part I, Structure of the Palisades Creek branch of the East Kaibab Monocline, Grand Canyon, Arizona: Memoir - Geological Society of America, no. 151, p. 235-271.

Stearns, D.W., 1978. Faulting and forced folding in the Rocky Mountains foreland. Laramide folding associated with basement block faulting in the western United States: Geological Society of America Memoir, v. 151, p.1-37.

Twiss, R. J., and Moores, E. M., 1992. Structural geology. W. H. Freeman and Company, New York.